CHALMERS
UNIVERSITY OF TECHNOLOGY

Functionalization of gold nanorods with Antimicrobial peptides

Department of Chemistry and Chemical Engineering

Mohamed Asaad

Applied Chemistry

CHALMERS UNIVERSITY OF TECHNOLOGY
Gothenburg, Sweden 2023
www.chalmers.se

Master's thesis 2023

Functionalization of gold nanorods with Antimicrobial peptides

Mohamed Asaad

CHALMERS
UNIVERSITY OF TECHNOLOGY

Department of Chemistry and Chemical Engineering

Applied Chemistry
Martin Anderssons Research group
Chalmers University of Technology
Gothenburg, Sweden 2023

Functionalization of gold nanorods with Antimicrobial peptides
Mohamed Asaad

© Mohamed Asaad, 2023.

Supervisor: Mats Hulander, Applied Chemistry
Examiner: Martin Andersson, Applied Chemistry

Master's Thesis 2023
Department of Chemistry and Chemical Engineering
Applied Chemistry
Martin Anderssons Research group
Chalmers University of Technology
SE-412 96 Gothenburg
Telephone +46 31 772 1000

Typeset in LaTeX
Printed by Chalmers Reproservice
Gothenburg, Sweden 2023

Department of Chemistry and Chemical Engineering
Mohamed Asaad
Applied Chemistry
Chalmers University of Technology

Abstract

Infections in biomedical implants can occur due to the growth of bacterial biofilms, and treating these infections becomes even more challenging due to problems such as antimicrobial resistance. Gold nanorods (NRs) provide an alternative approach to combating bacterial infections. When exposed to radiation, gold nanorods generate heat, which can be employed to eliminate bacteria. Antimicrobial peptides (AMPs) are naturally occurring peptides known for their potent ability to kill microorganisms. A combination between gold nanorods and AMPs could potentially show promising results and open up for new, safe and efficient treatment options of bacteria.

The primary objective of this study was to investigate the interaction between gold nanorods and antimicrobial peptides, focusing on optimizing the attachment of these peptides to the nanorods. Two distinct types of antimicrobial peptides were employed: one with a positive charge and another one terminated with thiol groups.

In the case of the positively charged antimicrobial peptide, it was observed that the removal of CTAB from the gold nanorods resulted in increased peptide attachment to the nanorods. Interestingly, it was also noted that the peptide not only bonded through thiol groups but also exhibited unfavorable attachment to the surface onto which the gold nanorods were coated, likely due to electrostatic interactions. To address this issue, two different strategies were applied. The first involved adjusting the pH of the system to induce electrostatic repulsion, while the second utilized a PEG silane polymer to block peptide attachment to the surface. Both approaches effectively reduced the amount of peptide binding to the surface. Additionally, introducing a pH of 11.5 with NaOH as the initial step in the QCMD measurement resulted in a cleaner silica surface, enhancing the attachment of various components.

For the thiol-terminated antimicrobial peptides, UV-Vis analysis revealed that these peptides exclusively attached to the surface through thiol bonding. Notably, A fascinating revelation came to light when exploring the temperature at which these peptides detached from the gold nanorods. Beyond 45°C, an additional resonance peak emerged at approximately 970 nm, adding an interesting dimension to the findings.

Keywords: gold nanorods, antimicrobial peptides, QCMD, thiol boding, resonance peak.

Acknowledgements

I'd like to begin by expressing my heartfelt gratitude to my supervisor, Mats Hulander, for his unwavering support, open-door policy, and invaluable insights throughout my research journey. My sincere appreciation also goes out to my examiner, Martin Andersson, for consistently providing me with ideas and guidance, helping me navigate the path forward.
I want to extend my thanks to Maja Uusitalo for her invaluable assistance in addressing various questions and challenges related to gold nanorods. Her contributions were instrumental in advancing my work.
Last but certainly not least, I would like to offer my deepest appreciation to my mother, whose support and love have been immeasurable. Words can hardly express the gratitude I feel for everything she has done.

Mohamed Asaad, Gothenburg, October 2023

List of Acronyms

Below is the list of acronyms that have been used throughout this thesis listed in alphabetical order:

AMP	Antimicrobial peptides
NR	Nanorods
QCMD	Quartz Crystal Microbalance with Dissipation
PEG	Polyethylene Glycol
PBS	Phosphate-Buffered Saline

Contents

List of Figures

1
Introduction

Biomedical implants have truly changed the game in the medical field. But, like all good things, they come with a downside. They can sometimes get infected, and these infections are actually one of the top issues we face when using such materials. Since they stay in the body for a long time, they present challenging infection issues. These infections are primarily attributed to bacterial biofilm growth. Biofilms are complex structures where bacteria adhere to surfaces and are surrounded by a protective layer of slime. The diagnosis of these infections can be complex, and treatment is further complicated by issues like antimicrobial resistance [1].

Antimicrobial drugs have played an essential role in decreasing death rates associated with infections over time. However, microorganisms, such as bacteria, have developed resistance to these drugs, making it difficult to treat such infections. As microorganisms become more resistant to antimicrobial drugs, the options for effective treatments become limited [13].

Gold nanorods (NR) offer an alternative treatment approach against bacteria. When irradiated with light of a specific wavelength, gold nanorods release heat, which can be used to kill bacteria. This heat is generated by the oscillation of free electrons on the surface of gold, known as localized surface plasmon resonance (LSPR). The shape and size of the nanoparticle determine the wavelength at which LSPR occurs. Gold nanorods are specifically used due to their plasmon resonance within the biological window, which falls in the near-infrared region. Light in this region can penetrate biological tissue and heat up nanorods, even those on implants, to eliminate bacteria [13].

Antimicrobial peptides (AMPs) are naturally occurring peptides found in plants, animals, and insects. They possess a high ability to kill microorganisms. A combination between gold nanorods and AMP could potentially show promising results and open up for new, safe and efficient treatment options of bacteria.This modification aims to enhance bacteria elimination by creating thiol bonds with gold nanorods. The combination of gold nanorods and AMPs holds potential for safe and efficient treatment options against bacteria. By heating the nanorods with light, the thiol bonds break, releasing the AMP. This dual effect of heat and the antimicrobial properties of the AMP contributes to bacteria elimination [13].

To study the functionalization of gold nanorods with AMPs, Quartz Crystal Microbalance with Dissipation monitoring (QCMD) will be used. This technique employs an oscillating quartz crystal as the sensor to measure the mass and thickness of the adsorbed layer when molecules are adsorbed onto the surface. The oscillation is generated through the piezoelectric effect when an electric field is applied to the crystal. Additionally, the shift in dissipation can be measured to determine viscoelastic properties. After functionalization, the gold nanorods will be exposed to near-infrared irradiation to eliminate bacteria [2].

Another technique utilized in this study is Scanning Electron Microscopy (SEM), which allows visualization of gold nanorod-covered surfaces and the eliminated bacteria. Furthermore, UV/VIS spectroscopy will be employed to quantify the amount of nanorods and spheres present in the gold solution.

1.1 Aim

The primary objective of this thesis is to explore the interactions between gold nanorods (NR) and antimicrobial peptides (AMPs). This exploration is driven by the overarching goal of enhancing the functionalization of AMPs with gold NR. AMPs are comprised of short sequences of amino acids. It's noteworthy that the specific type and arrangement of these amino acids play a pivotal role in shaping unique characteristics of AMPs and how they interact with gold nanorods.

Furthermore, we will investigate the critical aspect of the temperature at which AMPs detach from the surface, shedding light on an essential facet of this interaction.

1.2 Relevant Questions to answer

How can the number of AMPs attached to the gold NR be controlled or manipulated?

In what ways does the type of AMP influence its attachment to the gold nanorods? Are certain types of AMPs more effective or efficient in this regard?

What factors or conditions influence the strength of attachment between AMPs and gold NR? Are there any surface modifications or treatments that can enhance or weaken this interaction?

In the context of temperature, at what temperature or range of temperatures do AMPs typically detach from the surface of gold nanorods? Are there any temperature-dependent trends or patterns in this detachment process?

2

Theory

2.1 Gold nanorods

Gold nanorods are long gold nanoparticles with unique chemical, optical and electronic properties that make them beneficial in biomedical imaging, sensing, and catalysis applications. The synthesis process is highly sensitive and requires careful consideration of various factors, such as temperature, concentration, and pH. The synthesis of gold nanorods is carried out in two solution, seed and growth solution [14]. Figure 2.1 shows an illustration of the synthesis of the gold nanorods.

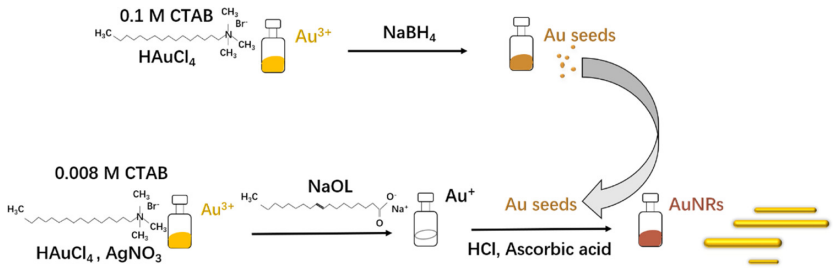

Figure 2.1: Schematic representation of the gold nanorods synthesis process [19].

2.1.1 Seed solution

In the seed solution small gold nanoparticles, that serve as nucleation sites where new gold atoms will deposit, are formed which subsequently leads to the elongation and formation of nanorods. The formation of gold nanoparticles is obtained through the reduction of gold ions. The seed solution consists of three components, a surfactant , gold salt and reducing Agent. Cetyltrimethylammonium bromide (CTAB) is often utilized as a surfactant whose task is to serve as a stabilizing agent in order to prevent nanoparticle aggregation and support uniform growth. It also plays role in controlling the anisotropic growth into nanorods. It achieves this by attaching itself to specific crystal facets on the growing nanorods, encouraging the longitudinal extension while inhibiting any expansion in other directions. When gold salt, often gold chloride ($AuCl_4^-$), is introduced, CTAB molecules will adhere to it and form layers around them. Subsequently, a reducing agent such as sodium borohydride ($NaBH_4$) is added to the solution to reduce the gold ions and form gold nanoparticles [14].

2.1.2 Growth solution

Once the seed solution has been prepared, it is combined with growth solution where gold nanorod growth takes place. Four components are used in the growth solution, gold salt, surfactant (CTAB),

silver nitrate, absorbic acid and hydrochloric acid. Silver nitrate is utilized to tailor and control the shape and size of nanorods when longer nanords are to be produced. Absorbic acid is a reducing agent that has a slower reduction kinetics than sodium borohydride. Through its slow reduction kinetics, absorbic acid plays a key role in controlling the rate of gold nanorods growth. Also and by having slow reduction kinetics, it enables controlled deposition of nanoparticles onto seed particles for controlled elongation of nanorods over time. The aim of using hydrochloric acid is to adjust the pH level in growth solution which is another crucial factor in controlling nanorods formation [14].

Figure 2.2: This illustration showcases how additives are employed to customize and regulate the shape and size of the gold nanorods [14].

2.2 QCMD

Quartz Crystal Microbalance with Energy Dissipation Monitoring (QCMD) is an analytical instrument for studying the absorption of thin films, interactions at surfaces or biomolecular interactions [2].

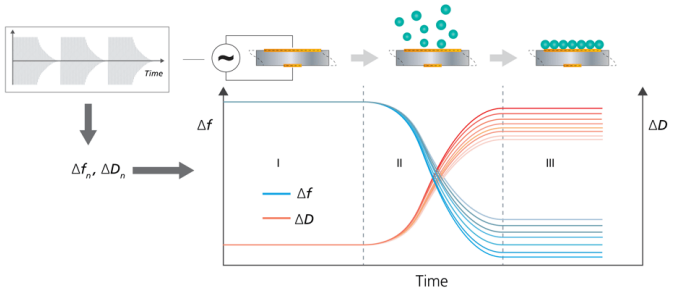

Figure 2.3: An illustration about the principle behind QCMD [15].

In QCMD, a quartz crystal resonator is used. The principle behind QCMD is to measure the change of the acoustic wave of the crystal as it vibrates at its resonance frequency. This is achieved by creating an electrode by covering the layer of quartz crystal with conductive materials. The crystal vibrates at its resonance frequency when an alternating current is applied. This resonance frequency depends on both thickness of crystal as well as elastic properties of quartz [2].

When mass is adsorbed onto the surface a shift in resonance frequency is observed. This shift is directly proportional to the amount of mass adsorbed on the surface. QCMD measures not only frequency variations, but also the energy dissipation during oscillation [2]. However, since the dissipation measurements are not relevant to the aim of this project, they will not be further explained.

2.2.1 The Sauerbrey equation

The Sauerbrey equation is an empirical relation named after Gerhard Sauerbrey who discovered that relation in 1959. The relation establishes a linear relation between the frequency shift and the mass change. The relationship is based on the assumption that the properties of the adsorbed film do not significantly impact the frequency shift as long as the film is rigid and much thinner than the acoustic wavelength. However, it is important to note that the Sauerbrey relation is not applicable when the dissipation change rate, represented by $\frac{\Delta D}{\Delta f}$, exceeds $4{\cdot}10^{-7}$ Hz^{-1} [16].

$$\Delta m = -S \cdot \frac{\Delta f}{n} \tag{2.1}$$

Where n is the number of the odd harmonic and S is called the sensitivity constant :

$$S = \frac{d_0 \cdot \rho_q}{f_0} \tag{2.2}$$

where ρ_q is the density of the quartz and d_0 is the thickness of the crystal. For a typical 5 MHz quartz crystal, it is known that $\rho_q = 2.65\,\mathrm{g/cm^3}$ and $d_0 = 334\,\mu\mathrm{m}$ that give $S = 17.7\,\mathrm{ng/Hz/cm^2}$. This gives the following equation:

$$\Delta m = -17.7 \cdot \frac{\Delta f}{n} \tag{2.3}$$

The thickness (nm) can then be derived as following:

$$thickness = (\frac{\Delta f}{n}) \cdot 10^{-2} \tag{2.4}$$

2.3 Scanning electron microscopy (SEM)

Scanning electron microscopy (SEM) is an extremely powerful tool that can be used for high-resolution imaging of sample surfaces in various fields. With a resolution as fine as 1.5 nm, it can provide information about topography, the surface features of an object, its texture, morphology, the shape and size of the particles, composition analysis when combined with energy Dispersive X-Ray Spectroscopy (EDS) and it can give crystallographic information. Figure 4.11 presents a schematic illustrating of the working principle of SEM [3].

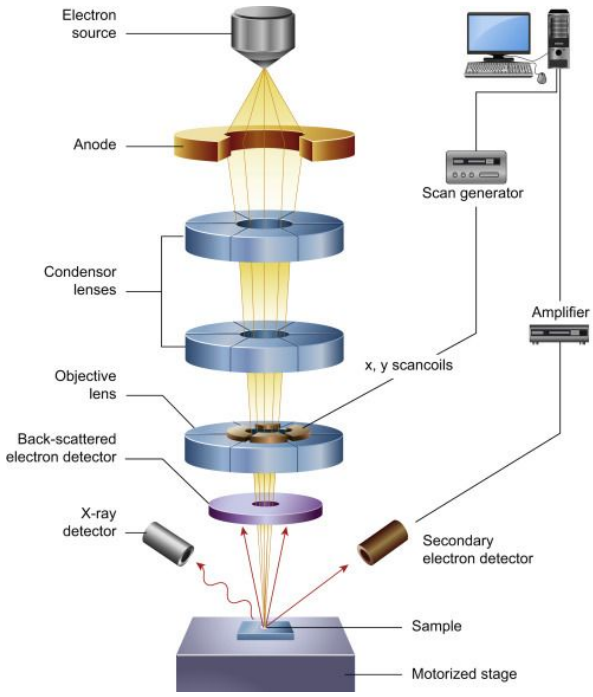

Figure 2.4: A schematic illustrating the working principle of SEM [8].

The electron are usually generated using field-emission gun (FEG) that produces electrons upon heating. The electron beam passes through a column consisting series of electromagnetic lenses that focus and control the beam's intensity, size and shape. It is crucial to maintain a vacuum within the column since gases could react with the electron source and burn it out, or it could cause electrons in the beam to ionize. Additionally, molecules present in the column could also hinder the transmission of the electron beam. When the electrons meet the sample, electrons from the sample will scatter due to different interactions between the incident beam and the sample [3], these interactions can be shown in figure 2.5.

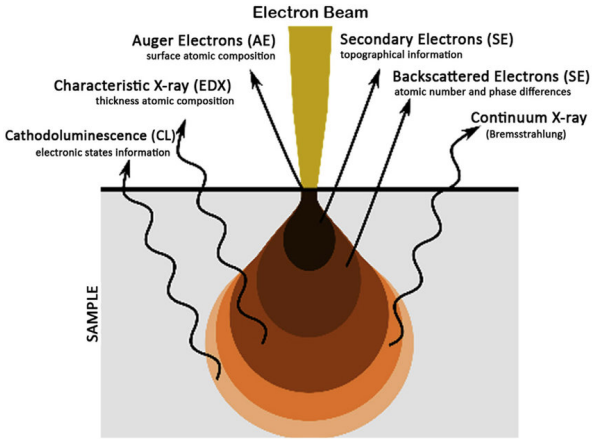

Figure 2.5: An illustration about how electrons from the sample will be will scattered due to different interactions between the incident beam and the sample when electrons meet the sample [4] .

The different interaction between the sample and the incident beam can be be categorized into two main types. The first one is elastic scattering where so called backscattered electrons (BSE) give topographical and phase information. The second one is inelastic scattering where secondary electrons (SE) provide the highest resolved topographical images and X-rays can provide information about the compositing of the sample. Subsequently, there are different types of detectors than can be utilized. However, the most common detectors are SE detectors, BSE detectors, and X-ray detectors that are used for elemental analysis [17].

2.3.1 UV-Vis

UV-Vis is a technique used to investigate the interaction between light and sample, specifically the absorption and transmission of light in the visible (Vis), ultraviolet (UV) region. The basic principle involves passing a beam through the sample and measure the amount of the sample that passes through. The degree of light absorption can be estimated using the following equation:

$$A = -log(T) = log(\frac{I_0}{I}) \tag{2.5}$$

where T is the transmittance, I is the intensity spectrum of light transmitted through a sample, I_0 the intensity spectrum of light transmitted through the blank [7].

2.4 Localised surface plasmon resonance

Nanoparticles can absorb photons and cause an oscillation at the surface of delocalised electrons. Photons and plasmons have similar quantisation, which will result in discrete levels of absorption. This, in turn, depends on the shape of the nanoparticle [5]. Figure 2.6 illustrates various possible nanoparticle shapes.

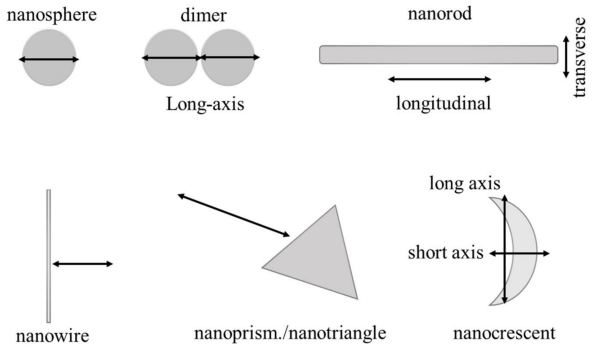

Figure 2.6: Illustrates various possible nanoparticle shapes. [5] .

As it can be seen in figure 2.6, nanorods are known to exhibit two LSPR. One exhibits a very strong polarisation along the nanorods' long axis. This is known as longitudinal LSPR. The other exhibits a very weak polarisation along the nanorods' short axis [5].

2.5 Refractive index

Localized surface plasmon resonance (LSPR) is highly sensitive to refractive index which is dimensionless number that measures the light-bending ability of a medium. It is defined as the ratio of the speed of light in a vacuum to the speed of light in the medium under consideration:

$$n = \frac{c}{v} \tag{2.6}$$

where: n is the refractive index, c is the speed of light in vacuum ($x \approx y$ 299,792,458 meters per second), and v is the speed of light in the medium [11]. The refractive index of a medium can change due to several factors like temperature, pressure, and optical density [12]. In this particular study, we're particularly interested in optical density. The attachment of AMPs to gold NR can change the way the particles are arranged and how tightly they're packed together. This, in turn, leads to a shift in the wavelength where LSPR, or localized surface plasmon resonance, shows up.

2.6 Thiol bonding

The thiol bonding of gold nanorods plays a pivotal role, especially when it comes to customizing the nanorods for a range of different uses. Thiol groups are particularly drawn to gold surfaces, and this forms the foundation of thiol-gold bonding. The sulfur atom in the thiol group (-SH) forms a semi-covalent bond with the gold atoms found on the nanorods' surface. This bond is quite stable and strong [9].

2.7 AMPs

Antimicrobial peptides (AMPs) are naturally occurring peptides found in plants, animals, and insects. They have a high ability to kill microorganisms.
In this study, two distinct types of antimicrobial peptides (AMPs) were employed. The first one is

known as CC-AMP, and it was intentionally designed in the laboratory by the company GenScript. Its sequence is as follows: CCRRPRPRPRPWWWW [10].

The second one is Polyphemusin which is a cationic antimicrobial peptide originating from the American horseshoe crab, Limulus polyphemus. This peptide is recognised for its potent antimicrobial properties, effectively targeting a wide spectrum of microorganisms, encompassing both Gram-negative and Gram-positive bacteria [13].

The amino acid sequence of this antimicrobial peptide is RRWCFRVCYRGFCYRKCR [10], and it's worth noting that the amino acid C (cysteine) is not positioned at the end of the sequence. This particular arrangement could potentially pose a challenge for the formation of the gold-thiol bond, given that cysteine is a key player in such bonding processes since it includes the -SH group.

3

Methods

3.1 Basic Piranha

It is a mixture of MQ-water, ammonia (NH_3) and hydrogen peroxide (H_2O_2) which is very reactive and is used to clean glass wares. A ratio of 4:1:1 was employed for these components. The glass wares were placed in the mixture which was heated for 30 minutes after the temperature had reached 80 °C. Then, the glass wares were rinsed carefully with MQ-water eliminate any remaining traces of the Piranha solution. Lastly, the glass wares were dried using nitrogen gas.

3.2 Synthesis of gold nanorods

3.2.1 Seed solution

This section will show the amount of substance that are needed in order to synthesise a 10 ml seed solution. The synthesis was performed in a water bath maintained at a temperature range of 27 °C to 30 °C. To initiate the synthesis, 25 µL $HAuCl_4$ (50 mM) was added to 4.7 mL CTAB (0.1 mM). The resulting solution was then stirred at 400 rpm for 5 minutes. Then, freshly prepared 300 µL $NaBH_4$ (10 mM) was added to the solution while vigorously stirring at more than 1400 rpm for a duration of 10-20 s. This resulted in an immediate change of color of the seed solution where a light brown color was obtained which can be seen in figure 3.1. After that, the solution was stirred at 400 rpm within the water bath at the desired temperature range of 27 °C to 30 °C in order to avoid CTAB crystallization.

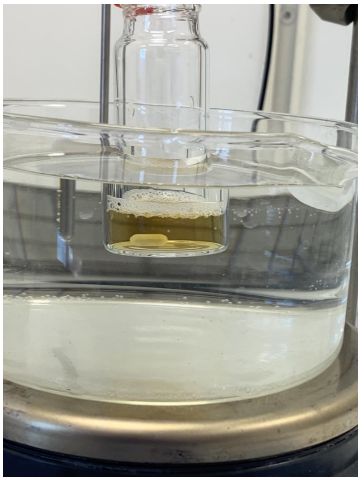

(a) The color of the seed solution before adding the $NaBH_4$.

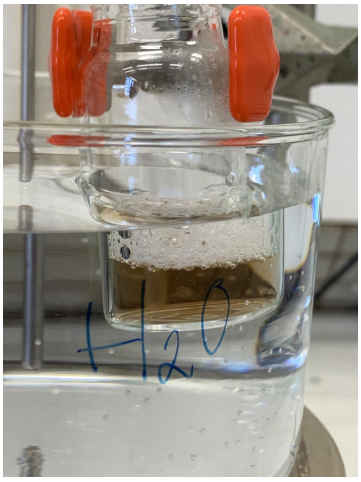

(b) The immediate change of color of the seed solution after adding the $NaBH_4$.

Figure 3.1: Seed solution.

3.2.2 Growth solution

This section will show the amount of substance that are needed in order to synthesise a 10 ml growth solution. The reaction took place in a water bath set to a temperature of 30 °C. 190 µL of HCl (1 M) and 100 µL of $HAuCl_4$ (50 mM) were added to 10 mL of CTAB (0.1 M). The resulting solution was gently stirred at 200 rpm for a few minutes. Then, 120 µL $AgNO_3$ (10 mM) was added to the solution. After a few seconds, 100 µL of ascorbic acid (100 mM) was added while the solution was stirred at 1000 rpm, turning the solution to a colorless solution. Finally, 25 µL of seed solution was added to the growth solution which was shaken by hand for a few seconds. The solution was then allowed to incubate for 2 hours in the 30 °C water bath.

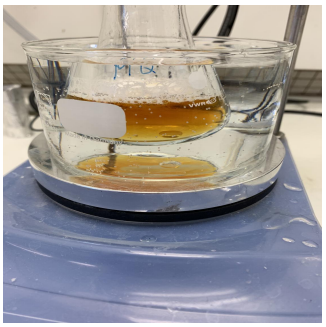

(a) The color of the growth solution before adding the absorbic acide.

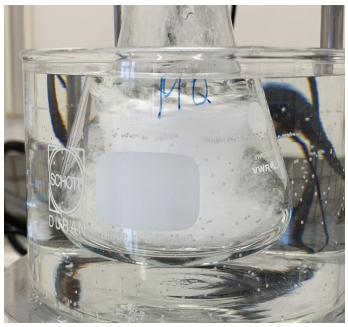

(b) The immediate change of color of the growth solution after adding absorbic acide.

Figure 3.2: Growth solution.

Figure 3.3 shows how the color of the gold nanorods solution change during two hours.

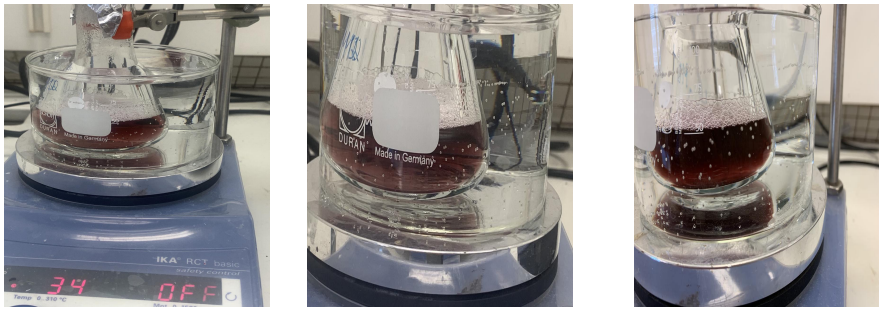

(a) The color of the gold solution after 30 minutes.

(b) The color of the gold solution after 60 minutes.

(c) The color of the gold solution after 2 hours.

Figure 3.3: Gold nanorods solution.

3.3 QCMD

3.3.1 Surface Modification

When it comes to QCMD, silicone dioxide sensors were used. The surfaces were first placed in a beaker filled with ethanol and the beaker was placed in the ultrasonic cleaner for 30 minutes at 25 °C, power setting of 2. Then, the sensors were cleaned with MQ-water, dried, and transferred to a UV-oven where they were exposed for 1 hour. The surfaces were then rinsed with MQ-water and immersed in a gold nanorods solution for two hours. After that, the surfaces were washed with ethanol and left to air-dry. To remove any remaining CTAB, the surfaces were placed in the UV-oven for one hour, and MQ-water was used once again to rinse the surface and remove any organic residues.

3.3.2 QCMD analysis

The flow rate used was $25\,\mu L\,s^{-1}$. The analysis began with the introduction of a PBS solution to establish a stable baseline. Once the baseline was achieved, NaOH (pH = 11.5) was injected into the system followed by another cycle of PBS. Then, AMP was introduced into the system and allowed to flow for 30 minutes. Finally, the system was flushed with PBS as the last step of the process.

3.4 Glass Surfaces

Glass surfaces were positioned within a holder and subjected to thorough cleaning using a basic piranha solution. Following this cleaning step, the surfaces were rinsed with MQ water, followed by gentle drying using nitrogen gas. Subsequently, they were exposed to ultraviolet (UV) radiation in the UV-oven for a duration of one hour. Following the UV treatment, the glass surfaces were once again rinsed with water and carefully dried using nitrogen gas.

After that, the surfaces were positioned within a specialized holder where up to nine surfaces can be added, which was then carefully placed into a cuvette. These cuvettes were subsequently filled with a 1.5 ml solution containing gold nanorods, allowing the surfaces to immerse for a period of two hours. Subsequent to this immersion, the cuvettes were cleansed using MQ-water. The holder,

housing the treated surfaces, was then transferred to a fresh cuvette, where a 1.5 ml solution of AMP was introduced and left to interact for one hour.

4

Results

Before proceeding to the analysis of the results, it is important to note that in some measurements SDS was used in order to study if the sensors can be cleaned after the the peptide attachment. However, the system behaved in an unexpected way which needs further studies that are not relevant to the aim of this project. Therefore, the obtained results regarding SDS will not be discussed in this report. It also should be noted that for the QCMD, the AMP polyphemusin was used.

Figure 4.1a illustrates QCMD measurements when bare silica surface is used. The aim behind using such a surface is to investigate whether the peptide binds to the surface surface onto which the gold nanorods is coated.

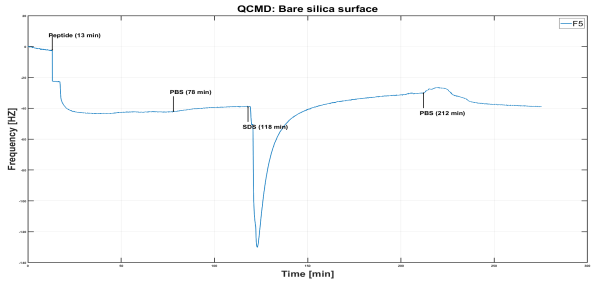

(a) QCMD measurements were conducted on bare silica surfacemonitor the frequency shift over time during the addition of various components. The fifth frequency was recorded for this measurement, as well as for all subsequent QCMD measurements.

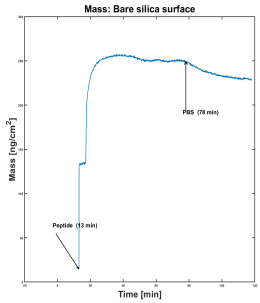

(b) The mass of the peptide immobilized on the surface.

Figure 4.1: Bare silica surface.

It is clearly seen that the peptide binds very quickly to the bare silica surface, around 225 ng/cm^2 (figure 4.1b). This is quite expected and has to do with the electrostatic interaction since the peptide is positively charged and the silica surface is negatively charged.

Now, for a silica surface coated with gold nanorods, as seen in figure 4.2, a greater mass of the peptide is binding to the surface, as depicted in figure 4.2. The increased mass binding can be attributed to the peptide binding not only to the silica surface via electrostatic interactions but also to the gold nanorods through thiol bonding. This dual binding mechanism results in a higher mass being detected by the QCMD measurements.

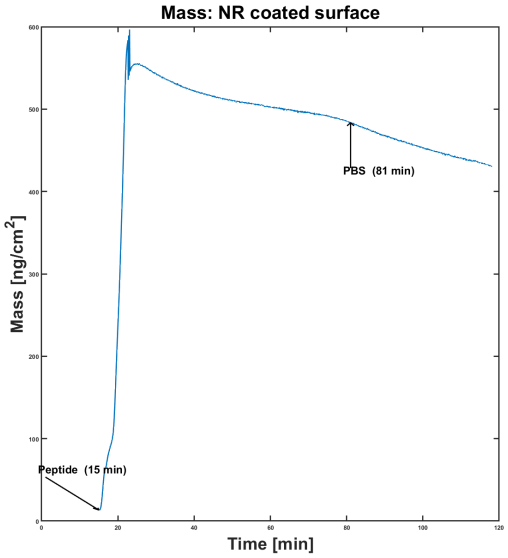

Figure 4.2: The mass of the peptide immobilized on silica surface coated with nanorods.

The presence of CTAB on gold nanorods can hinder the peptide from binding to the nanorods, therfore the CTAB has been removed utilizing ozon treatment of the sensor by placing it in an UV oven before starting the QCMD measurments than can be seen in figure 4.3.

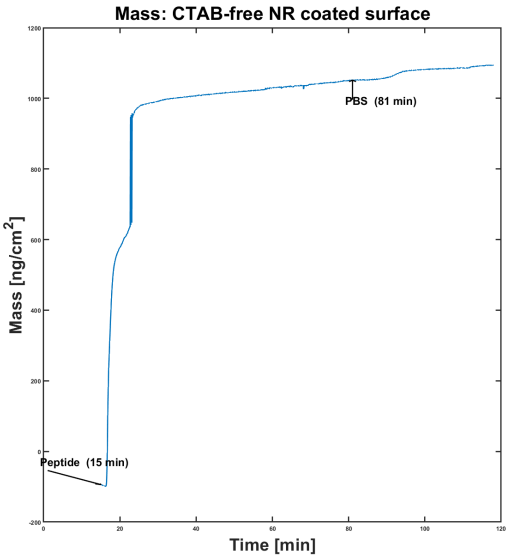

Figure 4.3: The mass of the peptide immobilized on silica surface coated with nanorods which, in turn, do not contain CTAB.

Comparing figure 4.2, where a surface with gold nanorods containing CTAB is used, with figure 4.3

where the CTAB has been removed from the nanorods, reveals that almost double mass attachment of the peptide is obtained for the later surface with nanorods without CTAB. The reason for the increase in mass attachment on the surface is that CTAB is a large molecule that covers large space of the nanorods. By removing the CTAB, the available surface area of the nanorods is increased which provides more space for the peptide to attache to the surface. As a result, in higher mass of the peptide is able to attach to the surface.

4.1 Interaction analysis

The attachment of the peptide to the surface onto which the gold nanorods is coated is not desired and should be avoided. Therefore, certain experiments have been conducted in order to study methods about how this type of attachment can be hindered or at least be reduced.

Since the peptide binds to gold nanorods through a gold-thiol bond and to the silica surface through electrostatic attraction, an idea is to increase the pH value of the system by one unit above the isoelectric point of the peptide polymphemuisn which is around 10.6 using NaOH (pH=11.5). In this case, the peptide will change its charge and become negatively charged which leads to repulsion form the negatively charged silica surface, thereby reducing the attachment to that surface. The idea is first to allow the peptide attache to the surface under same condition of the previous experiments and then, increase the pH of the system hence the attachment had occurred.

However, there is still a concern that the high pH to which the sensor is exposed could lead to etching away all silica from the surface. Therefor, this will be examined by adding NaOH to the surface as a first step to observe the extent of etching and then estimate if the etched amount could mean that all silica is cleaned away. By adding PBS as a second step, the system can then be brought back to the normal conditions used in the previous exterminates were performed.

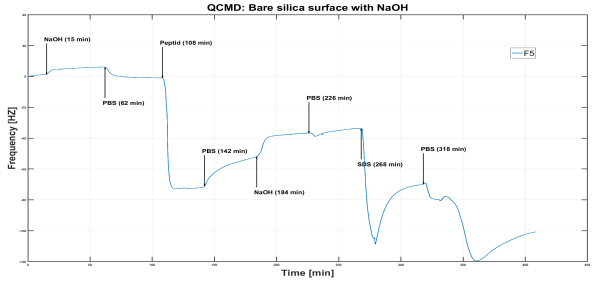

(a) QCMD measurements conducted on bare silica surface with NaOH . The measurment starts with the addition of NaOH to assess the extent of silica etching. Then, NaOH is added after the peptide to increase the pH of the system and the change the charge of the peptide. This was done to induce repulsion between the peptide and the silica surface, thereby reducing the attachment of the peptide to the surface.

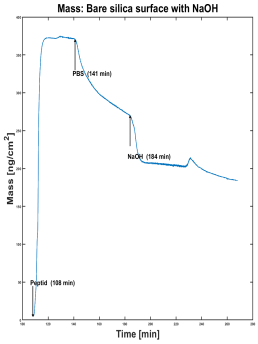

(b) The mass of the peptide immobilized on the silica surface.

Figure 4.4: Bare silica surface with NaOH.

As it is shown in figure 4.4b, almost more than 50% of the peptide is removed from the surface due to the addition of NaOH to the system which is quite a lot if we compare that with figure 4.1b where NaOH is not added to the system and where almost no peptide is removed from the bare silica surface.

Interestingly, the amount of the peptide that has been attached to the surface has doubled when NaOH is utilized. This may has to do with the fact that NaOH has cleaned the silica surface when it was introduced to the system creating more space for the peptide to bind to the bare silica surface.

Figure 4.5 shows how the mass (4.5a) and the thickness (4.5b) of the bare silica surface changes when adding the NaOH to the system as a first step. Unexpected results where no loss were obtained, on the contrary, a small amount of mass were gained. An explanation for this could be that the NaOH has cleaned the surface and removed any contaminants or impurities present on the surface, resulting in a clean and pristine surface. Consequently, when the PBS solution is introduced after the NaOH treatment, the ions from the PBS can readily bind to the surface, leading to a small gain in mass.

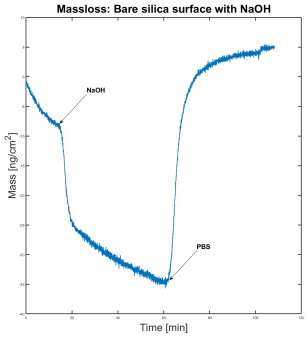

(a) Mass loss of bare silica surface when adding NaOH to the system as a first step.

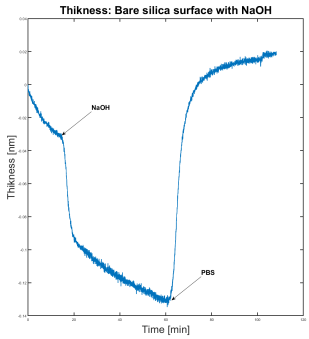

(b) Thickness loss of silica surface with NaOH when adding NaOH to the system as a first step.

Figure 4.5: Bare silica surface with NaOH.

The obtained results in figure 4.5 suggest that the NaOH treatment enhance the binding of AMP to the bare silica surface. Therefore and from now and on, NaOH will always be introduced to the system as a first step in order to clean the surface. Figure 4.6 shows another approach to hinder or reduce the interaction between the silica surface and the peptide. In this experiment, PEG silane where utilized to plock the peptide from interacting with the silica surface. The idea is to introduce the polymer before the peptide, in this case, the polymer occupies the available binding sites on the surface, making it difficult for the peptide to attach.

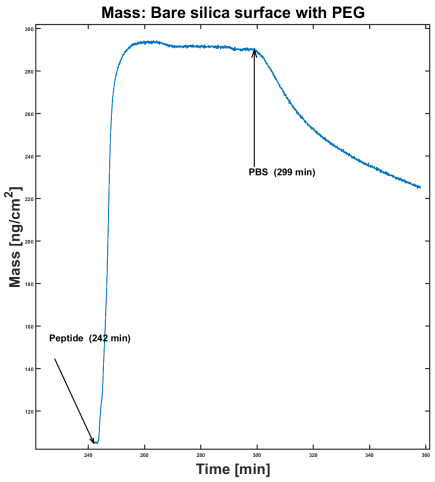

Figure 4.6: The mass of the peptide immobilized on the silica surface with addition of PEG silane with prior to peptide.

It can be seen in figure 4.6 that a net peptide attachment of 150 $\frac{ng}{cm^2}$ is obtained which much lower than that when NaOH was used , 200 $\frac{ng}{cm^2}$ (see figure 4.4b). This suggests that the PEG acts as a blocking agent, preventing the binding of the peptide to the silica surface.

The next step is to examine a silica surface coated with gold nanorods without CTAB, in the presence of PEG. As soon as NaOH is introduced to the system as first cleaning step, a big mass loss is obtained as it can be seen in figure 4.7. This indicates that that the coated nanordos on the surface is cleaned away by the NaOH. The high pH of the NaOH solution led to detachment of the nanorods from the surface. The loss indicate that the nanorods are susceptible to the NaOH treatment.

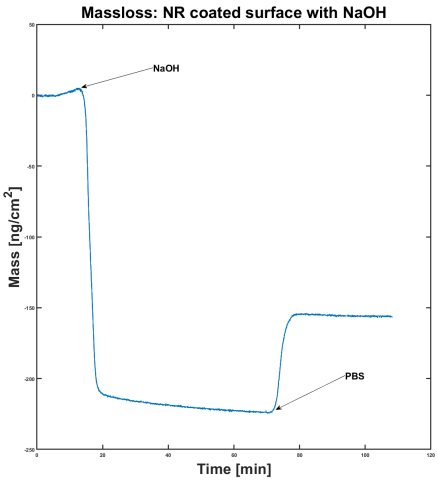

Figure 4.7: Gold nanorods coated surface with addition of PEG silane. The figure shows the mass loss on the surface due to the cleaning step with NaOH

In another experiment, figure 4.8 where nanorods coated silica surface was used, no such loss was obtained. A small loss that can be seen as a mass loss in figure 4.8b.

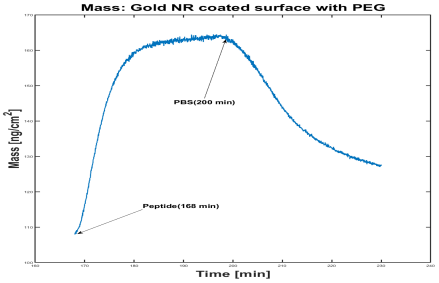

(a) The mass of the peptide immobilized on nanorods coated surface with the addition of PEG prior to the peptide.

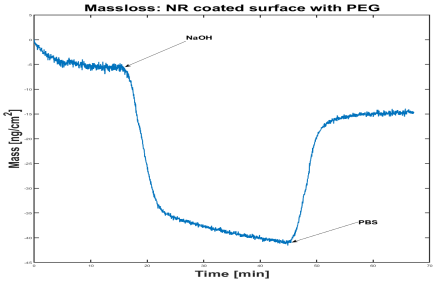

(b) Mass loss nanorods coated surfce with addition of PEG when introducing NaOH to the system.

Figure 4.8: Gold nonorods coated surface with addition of PEG silane prior to the peptide. The experiment was conducted similarly to figure 4.7. However, the sensors in this experiment was treated in different way. The sensor has not been washed with MQ-water after the O_3 treatment which in turn is done in order to remove the CTAB, but it was directly transferred from the oven to the QCMD machine without undergoing additional rinsing steps.

It is seen in figure 4.8b that there is minimal mass loss of the gold nanorods when NaOH is used which indicates that NaOH is not very suitable for the surfaces coated with gold nanorods. However, this could also depend on the application and on how the these surfaces are going to be used, such small loss may not have big influence on the results in some applications.
Why less mass loss is obtained in this experiment is still unknown and needs further investigations. On other hand, it should be noted that the sensor, used in this experiment showed in figure 4.8, was treated in a different way where the sensor was not washed with MQ-water after the removal of CTAB in the UV-oven, it was placed directly in the QCMD machine. Perhaps, there are still some organic rests on the sensor that some how helps the gold nanorods to stick strongly to the surface and not be affected by the NaOH. The other reason that could play role is the time gap between surface functionalization and QCMD measurements (7 days in this experiment) could also play a role in the observed behavior. But as it is mentioned above, this behaviour needs further studies.

The last experiment showed in figure 4.9, was done utilizing silica surface coated with gold nanorods without CTAB and no NaOH treatment was applied. This is in order to compare the results with the previous experiments where no NaOH was used.

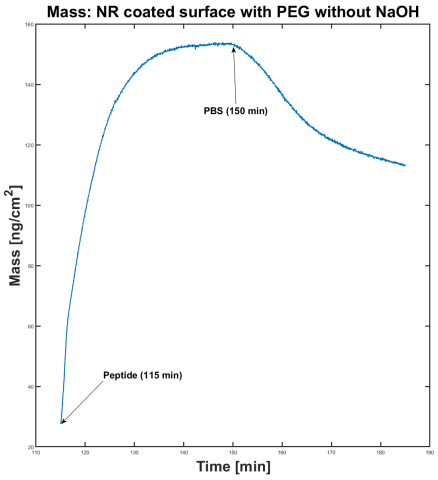

Figure 4.9: The mass of the peptide immobilized on nanordos coated surfce with addition of PEG prior to the peptide. QCMD measurements were performed on nanorods coated surfce without CTAB and no NaOH treatment was applied and with addition of PEG silane

As it can be seen in figure 4.9, less amount of peptide are adsorbed to the surface than the experiment where NaOH was used as cleaning step, see figure 4.8a. This has to do with the fact that NaOH cleans the surface and create more space for the peptide to bind. Furthermore, some of the gold nanorods were washed away from the surface when NaOH was used which, in turn, creates more space for the peptide to bind to the surface. Also, 90% decrease in peptide attachment is obtained compared to the experiment showed in figure 4.3 where no PEG is used. This results means that the PEG blocks both the silica surface and the gold nanorods.

Figure 4.10 shows the UV-VIS spectroscopy of the gold nanorods solutions that were synthesised in the lab.

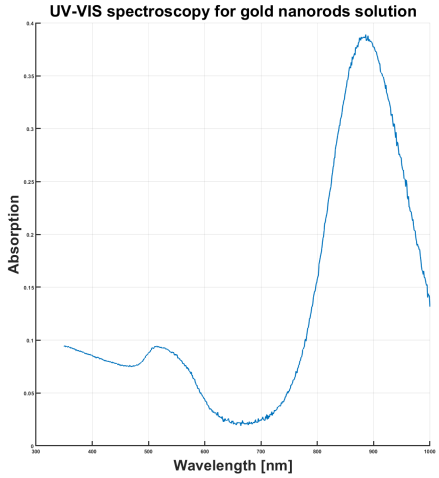

Figure 4.10: UV-VIS spectroscopy for gold nanorods solution

As seen in figure 4.10, the synthesised gold nanorods exhibit a marked absorbance peak at wavelengths around 900 nm as well as a smaller peak around 500 nm. By making attention to the sharp peak at wavelength 900 nm where gold nanorods show its plasmonic behaviour, one can clearly see that gold nanorods have been synthesised successfully . Another peak is also obtained near 500 nm indicating the other shapes such gold nanosphers have also been built. This result is quit expected and in order to get solutions that only includes gold nanorods, special equipment, that are not provided in our lab, need to be used.

Figure 4.11 shows a picture of SEM analysis of the a silica surface coated with gold nanorods. The obtained results further supports the results obtained from the UV-Vis. The SEM image confirms the presence of both nanorods, this is correlated with the peak at 900 nm, and other shapes that are correlated with the peak around 500 nm.

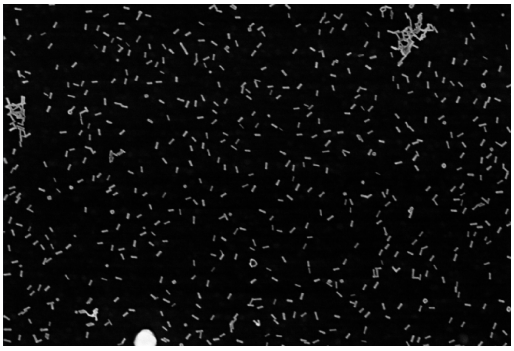

Figure 4.11: SEM analysis of a surface coated with gold nanorods.

4.2 Interaction analysis, glass surfaces

It's important to highlight that, In this section, the utilized AMP is CC-AMP, which is thiol-terminated.

As observed, QCMD is a possible technique for studying surface interactions. However, it wasn't originally designed for this type of analysis. Additionally, the silicon dioxide sensors come at a high cost. Therefore, moving forward, interaction analyses will be conducted on glass surfaces using UV-Vis spectroscopy.

The study of interaction analysis began with understanding the system. Multiple experiments were conducted to optimize the concentration of gold nanorods coated on the surface. Various methods were employed, including increasing the number of surfaces in each sample and using a more concentrated gold nanorods solution. Additionally, longer incubation time of the surfaces to the gold nanorods were also evaluated.

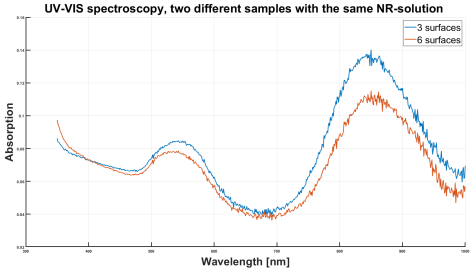

(a) UV-VIS spectroscopy for two distinct samples: the first sample has 6 surfaces, while the second has 3 surfaces. The same solution was applied to both samples.

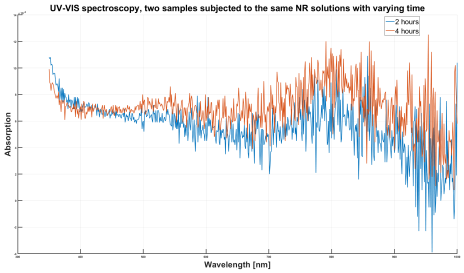

(b) Two distinct samples exposed to the same gold nanorods solution for 2 hours and 4 hours, respectively.

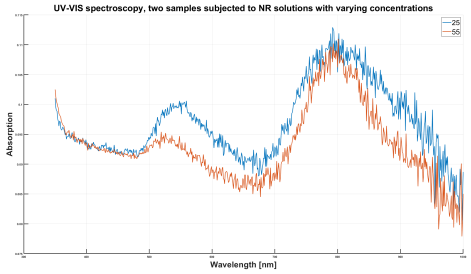

(c) Two samples were exposed to NR solutions of varying concentrations. The same base solution was used, and different concentrations were achieved by diluting it.

Figure 4.12: Examines the concentration of nanorods adhered to a surface.

While one might assume that an increased number of surfaces would result in a higher signal due to more interaction area, and consequently, a larger number of gold nanorods coated on the surface, experimental results did not support that. There was no noticeable pattern indicating how the number of surfaces might influence the resulting signal. Figure 4.12a illustrates an example where a sample with a greater number of surfaces produced weaker signals.

No correlation between the concentration of nanorods in the solution and the number of nanorods adhering to the surface was found. Figure 4.12c demonstrates a scenario where a higher concentration resulted in a reduced signal, implying fewer gold nanorods coated on the surface.

The primary factor influencing the quantity of gold nanorods on the surfaces appears to be the exposure duration to the gold nanorods solution. An extended exposure time consistently led to an increased number of gold nanorods being coated on the surface.

Another experiment aimed at getting a deeper understanding of the system involved functionalizing glass surfaces coated with gold nanorods with AMP and subsequently storing them in a refrigerator for a duration of six days. UV-Vis measurements were performed on days one, two, and six of the storage period, and no changes were observed. This suggests that the samples can be stored for a long period if necessary, as demonstrated in Figure 4.13.

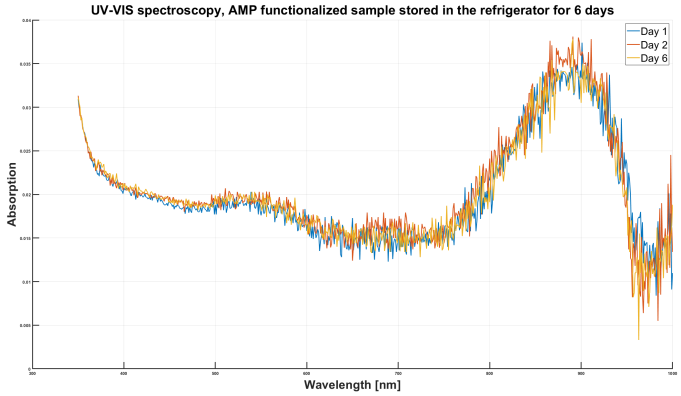

Figure 4.13: UV-Vis spectroscopy results for a surface coated with gold nanorods functionalized with AMP, which were stored in the refrigerator for 6 days.

The next step involves investigating the binding of the peptide to the gold nanorods. Glass surfaces coated with gold nanorods were exposed to the AMP solution for one hour, and various measurements were conducted throughout this duration to obtain a real-time analysis of the attachment of AMP molecules to the surface as it can be seen in figure 4.14.

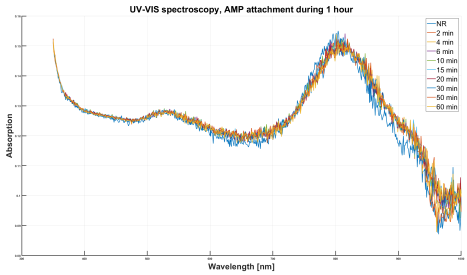

(a) UV-Vis spectroscopy measurments that illustrates the attachment of AMP on a glass surface that's coated with gold nanorods, observed within a one-hour timeframe.

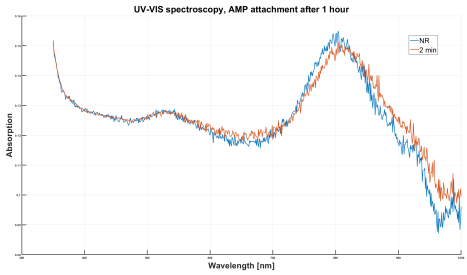

(b) UV-Vis spectroscopy of a glass surface coated with gold nanorods, both before and 1 hour after the addition of AMP.

Figure 4.14: AMP attachment on a surface coated with gold nanorods.

Figure 4.14 shows how the AMP:s attach to a glass surface coated with gold nanorods. The shift in the peak at 900 nm suggests that the antimicrobial peptides have bound to the gold nanorods. This binding interaction causes a change in the local refractive index or the electronic environment surrounding the nanorods, resulting in a shift in the plasmon resonance wavelength. The consistent absorbance at 900 nm indicates that the peptides did not displace or detach the nanorods from the glass substrate [18].

A shift in absorption with a change in intensity could be indicative of nanorod aggregation or reorientation upon peptide binding. Aggregation of the nanorods can alter their plasmonic properties, leading to changes in absorption and spectral features. If the absorption decreases, it might imply that aggregation has occurred, causing a reduction in the effective number of nanorods contributing to the signal. Conversely, an increase in absorption could indicate reorientation or dispersion of the nanorods due to peptide binding. However, in other experiments a shift associated with an increase in the absorption was observed [18].

The subsequent phase involves examining whether the AMP will detach from the gold nanorods upon heating. This investigation is crucial because the underlying objective of this project is to employ the gold nanorods and AMP for implant applications, followed by exposure to NIR (Near-Infrared) light to utilize the heating effect of plasmon resonance and the antimicrobial capabilities of AMP. Figure 4.15 illustrates the UV-vis spectroscopy measurements taken from samples comprising glass surfaces coated with gold nanorods that have been functionalized with AMP.

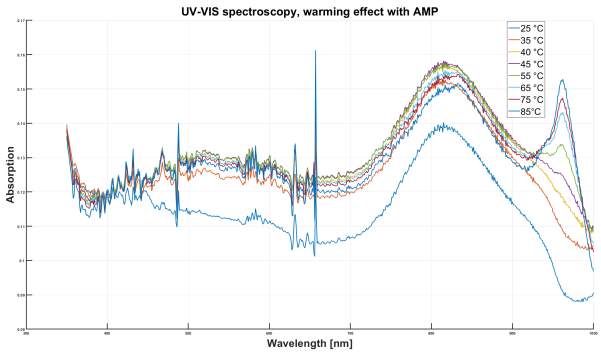

(a) The warming effect on glass surfaces layered with gold nanorods and then coated with AMP, as the temperature was progressively raised from 25°C to 85°C.

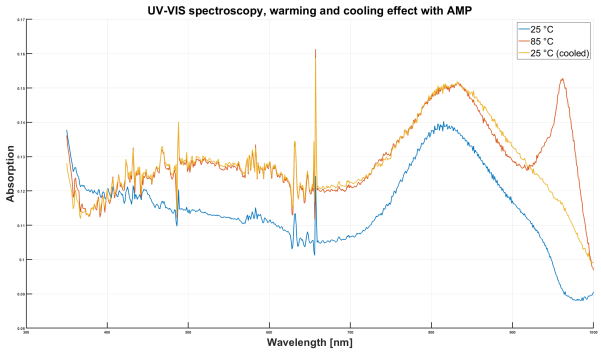

(b) The system's response when the temperature is reduced back to 25°C after being warmed up to 85°C.

Figure 4.15: UV-Vis spectroscopy measurements illustrating the warming effect observed on glass surfaces that are coated with gold nanorods and subsequently layered with AMP.

An additional resonance peak appears at approximately 970 nm when the temperature reaches around 45 °C, and it becomes more distinct and well-defined with increasing temperature. A similar pattern was observed in a different study [6] when the temperature was elevated to 53 °C. It could be argued, as demonstrated in this study [6], that this new peak is a consequence of changes in the geometrical configuration of the nanorods, influencing the wavelength at which gold nanorods exhibit localized surface plasmon resonance.

However, this explanation is contradicted by the disappearance of the additional peak at 970 nm when the temperature is subsequently lowered to 25 °C as illustated in figure 4.15b. An alternative explanation for this phenomenon could be the aggregation of gold nanorods when the temperature rises. It is also important to consider that the gold nanorods are functionalized with AMPs, which may potentially influence this behavior. Nevertheless, a control experiment was conducted using only glass surfaces coated with gold nanorods, and the same behavior was observed.

To explore whether the AMP attached to the surface has any impact on the appearance of the additional peak illustrated in Figure 4.15 and to validate the unexpected reversible behavior demonstrated in Figure 4.15b, we conducted another experiment, figure 4.16, on gold nanorods-coated surfaces without any AMP attachment.

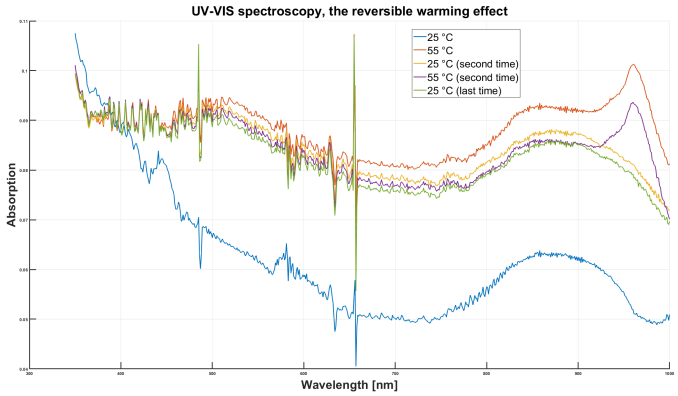

Figure 4.16: UV-Vis spectroscopy measurements illustrating the warming effect observed on glass surfaces that are coated with gold nanorods without any layering with AMP. The temperature was raised and lowered multiple times to investigate the reversibility phenomenon.

A similar behaviour, in figure 4.15, is obeserved when a gold nanorods-coated surfaces without any AMP attachment is used. This suggests that AMP does not influence the additional peak observed around 1000 nm. Figure 4.16 verifies the reversible nature of this behavior, although the underlying reason remains unexplained. This aspect warrants further investigation in future research studies.

The final phase of this project is to investigate the impact of NaOH on the gold nanorods and attempting to establish a correlation with the results obtained from the initial QCMD measurements. Figure 4.17 illustrates the use of two samples for this purpose: the first sample consists of glass surfaces coated with gold nanorods, while the second sample comprises glass surfaces coated with gold nanorods functionalized with AMP.

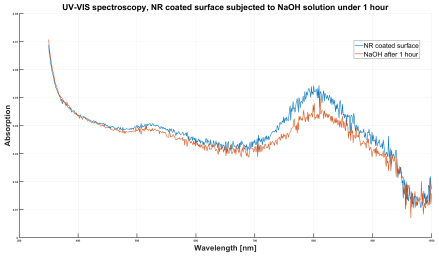

(a) Glass surfaces with gold nanorods without AMP functionalization. These surfaces underwent exposure to a NaOH solution with a pH of 11.5 for one hour

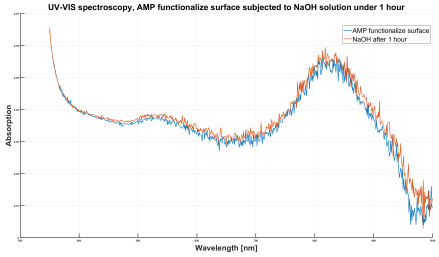

(b) Glass surfaces with gold nanorods that are functionalized with AMP. These surfaces underwent exposure to a NaOH solution with a pH of 11.5 for one hour.

Figure 4.17: UV-Vis spectroscopy results for a sample that was immersed in NaOH for a duration of 1 hour.

Figure 4.17a illustrates a decrease in intensity around 900 nm when the sample is exposed to NaOH(ph=11.5), where gold nanorods exhibit their plasmonic behavior. This reduction suggests a loss of some gold nanorods. This behavior aligns with what was observed in Figure 4.8, where a minor loss of gold nanorods occurred when the sample was exposed to NaOH at pH=11.5.

Neither decrease in peak intensity or a shift is not observed, when gold nanorods coated with AMP are immersed in a NaOH solution, as showed in Figure 4.17b. This behavior contrasts with the QCMD measurement results, where a silica sensor coated with gold nanorods functionalized with AMP was exposed to NaOH, as discussed in Figure 4.4a. In that scenario, some of the AMP molecules detached from the surface when exposed to NaOH.

Furthermore, unlike the positively charged AMP used in Figure 4.4a, where an electrostatic interaction occurs between AMP and the surface onto which the gold nanorods are coated, the AMP utilized in Figure 4.17b is thiol-terminated. This implies that there is no electrostatic interaction between the surface and the AMP, and the AMP molecules only attach to the gold nanorods via thiol bonding.

4.3 Summary

The project aimed to study the functionalization of gold nanorods with an antimicrobial pepitde to enhance bacteria elimination. A such functionalization was possible due to the thiol bonding between the nanorods and the peptide. However, unfavorable electrostatic interaction was observed between the peptide and the surface onto which the nanorods are coated.

To overcome this interaction, NaOH was used to change the pH value of the system, and change the charge of the peptide to enforce electrostatic repulsion. This was shown to be a good approach to reduce this interaction. Furthermore, two different behaviour, regarding the gold nanorods on the surface, were obtained when NaOH was used. The first one is that all nanorods were washed away where a small amount of the nanorods were affected in the second case. This behaviour need further investigation, however, two possible factors could contribute to this behaviour. The first one the approach that is used to coat the gold nanorods on the surface and the other one is the time between which the rods were coated on the surface to the time where the QCMD measurement was performed.

Another apporach, that was investigated in order to hidnder the interaction between the peptide and the surface onto which the nanorods are coated, is adding PEG silane to block the peptide from binding to the surface. It could be shown that using PEG silane reduced the amount of the peptide that is binding to the surface. However, it remains unclear whether PEG hinders the peptide form attaching to the silica surface, gold nanorods or both.

It was also shown that removing the CTAB from the gold nanorods led to that more peptide were able to attach to the surface since the CTAB is a large surfactant that covers the nanorods, and by removing it, more space is available to the peptide to bind to.

Another interesting finding in this project is the NaOH cleaning step.It was demonstrated that adding NaOH at pH=11.5 to the sensor that is used in QCMD, will clean that surface and allow more components to bind into it.

Regarding the quantity of nanorods that can be coated on a surface, the primary determining factor is the duration for which the gold nanorods are immersed in the gold nanorod solution. Longer immersion times resulted in a greater quantity of gold nanorods on the surface. Other factors, such as concentration, did not have any noticable impact in this regard. Also, it was showen that glass surfaces coated with gold nanorods functionalized with AMP can be safely stored in the refrigerator for an extended duration without any negative effects on their properties.

Both QCMD and UV-Vis analyses revealed that AMP binds directly to the gold nanorods within a remarkably short time of just 2 minutes.

Exposing glass surfaces to temperatures exceeding 45°C resulted in the appearance of an additional resonance peak at approximately 980 nm. Notably, this peak dissaperas upon lowering the temperature below 45°C. The experiment showed that this behavior is reversible, allowing for a back-and-forth transition. One possible explanation for this phenomenon is that the gold nanorods tend to approach each other and potentially aggregate at higher temperatures.

4.4 Future work

The impact of NaOH on the detachment of gold nanorods, expanding upon our findings has to be investigated

A compelling avenue for research would be to unravel the origins of the unexpected resonance peak observed when heating the samples.

Experiments at temperatures exceeding 85 °C to gain deeper insights into the detachment of AMP from gold nanorods.

Explore methods for altering the charge of the silica surface, such as using HCl, to disrupt AMP-silica interactions rather than modifying the AMP itself.

To further validate the specificity of thiol-terminated AMP for gold nanorods, incoming students could conduct QCMD measurements on a bare silica surface. This will help ensure that this type of AMP exclusively binds to gold nanorods in this system

5

Conclusion

It was observed that the removal of CTAB from the gold nanorods resulted in increased peptide attachment to the nanorods. Interestingly, in the case of the positively charged antimicrobial peptide, it was also noted that the peptide not only bonded through thiol groups but also exhibited unfavorable attachment to the surface onto which the gold nanorods were coated, likely due to electrostatic interactions. Additionally, introducing a pH of 11.5 with NaOH as the initial step in the QCMD measurement resulted in a cleaner silica surface, enhancing the attachment of various components.

For the thiol-terminated antimicrobial peptides, these peptides exclusively attached to the gold nanorods through thiol bonding. Notably, A fascinating revelation came to light when exploring the temperature at which these peptides detached from the gold nanorods. Beyond 45°C, an additional resonance peak emerged at approximately 970 nm. What's particularly noteworthy is that this extra resonance peak disappear when the temperature is reduced to 25°C and the both the appearance and the disappearance of the this resonance peak is reversible

Bibliography

[1] Carla Renata Arciola, Davide Campoccia, and Lucio Montanaro. Implant infections: adhesion, biofilm formation and immune evasion. *Nature reviews microbiology*, 16(7):397–409, 2018.

[2] Qian Chen, Shengming Xu, Qingxia Liu, Jacob Masliyah, and Zhenghe Xu. Qcm-d study of nanoparticle interactions. *Advances in Colloid and Interface Science*, 233:94–114, 2016. Clayton Radke Festschrift.

[3] Carleton College. Scanning electron microscopy (sem). `https://serc.carleton.edu/research_education/geochemsheets/techniques/SEM.html`, 2023.

[4] M. Ezzahmouly, A. Elmoutaouakkil, M. Ed-Dhahraouy, H. Khallok, A. Elouahli, A. Mazurier, A. ElAlbani, and Z. Hatim. Micro-computed tomographic and sem study of porous bioceramics using an adaptive method based on the mathematical morphological operations. *Heliyon*, 5(12):e02557, 2019.

[5] Pritam Khan, Grace Brennan, James Lillis, Syed A. M. Tofail, Ning Liu, and Christophe Silien. Characterisation and manipulation of polarisation response in plasmonic and magneto-plasmonic nanostructures and metamaterials. *Symmetry*, 12(8), 2020.

[6] Ramesh Marasini, Arunkumar Pitchaimani, Tuyen Duong Thanh Nguyen, Jeffrey Comer, and Santosh Aryal. The influence of polyethylene glycol passivation on the surface plasmon resonance induced photothermal properties of gold nanorods. *Nanoscale*, 10(28):13684–13693, 2018.

[7] Mettler-Toledo. Uv/vis spectroscopy explained. `https://www.mt.com/us/en/home/applications/Application_Browse_Laboratory_Analytics/uv-vis-spectroscopy/uvvis-spectroscopy-explained.html#absorbance`, 2023.

[8] Author's name. Application of nanomaterials in environmental improvement. *Journal Name*, Volume number(Issue number):Page range, Year of publication.

[9] N.d. Conjugation of oligonucleotides to gold nanoparticles, 2023.

[10] N.d. Genscript - make research easy - the leader in molecular cloning and gene synthesis, peptide synthesis, protein and antibody engineering, 2023.

[11] N.d. Refractive index, 2023.

[12] N.d. Refractive index: Definition and measurement, 2023.

[13] Maria Pihl, Ellen Bruzell, and Martin Andersson. Bacterial biofilm elimination using gold nanorod localised surface plasmon resonance generated heat. *Materials Science and Engineering: C*, 80:54–

58, 2017.

[14] Leonardo Scarabelli, Ana Sánchez-Iglesias, Jorge Pérez-Juste, and Luis M. Liz-Marzán. A "tips and tricks" practical guide to the synthesis of gold nanorods. *The Journal of Physical Chemistry Letters*, 6(21):4270–4279, 2015. PMID: 26538043.

[15] Biolin Scientific. Qcm-d - what is qcm-d? `https://www.biolinscientific.com/measurements/qcm-d#what-is-qcm-d`, 2023.

[16] Biolin Scientific. The sauerbrey relation. `https://www.biolinscientific.com/hubfs/Content%20Offer/QSense/EN/The%20Sauerbrey%20relation%20v2.pdf?hsLang=en`, 2023.

[17] Thermo Fisher Scientific. Scanning electron microscope (sem) electron column. `https://www.thermofisher.com/se/en/home/materials-science/learning-center/applications/scanning-electron-microscope-sem-electron-column.html`, Year of publication.

[18] Sirimuvva Tadepalli, Zhifeng Kuang, Qisheng Jiang, Keng-Ku Liu, Marilee A Fisher, Jeremiah J Morrissey, Evan D Kharasch, Joseph M Slocik, Rajesh R Naik, and Srikanth Singamaneni. Peptide functionalized gold nanorods for the sensitive detection of a cardiac biomarker using plasmonic paper devices. *Scientific reports*, 5(1):16206, 2015.

[19] Ming-Zhang Wei, Tian-Song Deng, Qi Zhang, Zhiqun Cheng, and Shiqi Li. Seed-mediated synthesis of gold nanorods at low concentrations of ctab. *ACS Omega*, 6(13):9188–9195, 2021. PMID: 33842787.

Department of Chemistry and Chemical Engineering
CHALMERS UNIVERSITY OF TECHNOLOGY
Gothenburg, Sweden
www.chalmers.se

CHALMERS
UNIVERSITY OF TECHNOLOGY